

Silica diagenesis in Eocene carbonates of the Okçular Formation, Turkey: inferences from field observations and petrography

Meryem YEŞİLOT KAPLAN^{1, *}

¹ İskenderun Technical University, Faculty of Engineering and Natural Sciences, Department of Petroleum and Natural Gas Engineering, Hatay, Turkey; ORCID: 0000-0001-8900-8823



Yeşilot Kaplan, M., 2025. Silica diagenesis in Eocene carbonates of the Okçular Formation, Turkey: inferences from field observations and petrography. *Geological Quarterly*, **69**, 30; <https://doi.org/10.7306/gq.1803>

The silica diagenesis of limestones depends on the environmental conditions and the presence of a silica source. Microstructural features, cracking, porosity, crystal/grain size and the chemical composition of the limestones and chert nodules and layers in the Okçular Formation are parameters controlling silica diagenesis. Cherts are observed in three forms (1) chert nodules with/without a rim, (2) fractured cherts, and (3) layered cherts. Authigenic quartz crystals, chertified foraminifers, microlaminations in the limestones and the chert-limestone grain size relation indicate diagenetic replacement. There is a positive correlation between the size of the microquartz crystals and the colour of the cherts, according to fluid circulation, the trace element content, and the degree of silicification. As the size of microquartz crystals increases due to all these factors, the colour changes from brown to grey-black. Crack widening due to nodule growth, the generally parallel arrangement of chert nodules in carbonates to cracks, and the presence of diagenetic stylolites indicate that both tectonic and diagenetic fractures played a role in silicification. The presence of Cl, P, Ti, Mn and Mo in the chertified zones in limestones indicates inorganic silicification in a marine environment.

Key words: chert, diagenesis, SEM-EDS, stylolite, carbonates.

INTRODUCTION

The term chert is used to describe a chemically deposited sedimentary rock composed mostly of microcrystalline quartz, chalcedonic quartz, and subordinate macrocrystalline quartz. Flint, a sub variety of chert, is described as “a very compact, dark grey, siliceous rock” (Glock, 1920). “Flint” is usually applied by archaeologists and refers mostly to silica concretions/nodules. Archaeologists employ different cutting-edge analytical methods as markers of flint artifact provenance (e.g., Kochman et al., 2020b; Migaszewski et al., 2022). According to some researchers, the distinction between chert and flint is based on the mineralogical composition in terms of silica polymorphs, but it is also common to use the term flint for black silica formations (Jurkowska and Świerczewska-Gładysz, 2020).

The origin of cherts is still debated. Formation models of chert nodules include: organic matter oxidation (Siever, 1962; Heath, 1974; Kastner, 1981; Hein and Koski, 1987); formation due to increased silica from volcanism (Yool and Tyrrell, 2005);

hydrogen sulphide oxidation (Clayton, 1986; Maliva and Siever, 1988); silica released during smectite-illite transformation (Metwally and Chesnokov, 2012); and formation in the mixing zone (Abdel-Wahab and El-Younsy, 1999; Hussein and Abd El-Rahman, 2020). The origin of cherts remains a poorly understood problem of recent geology. The delivery of silicon to the basin is a fundamental process that leads to the formation of flint on a large scale. This process involves the following basic mechanisms:

1 – riverine inputs of silica into a sedimentary basin (Tréguer et al., 1995);

2 – a mixing sea water-fresh water model proposed by Knauth and Epstein (1976) and described also by Hussein and Abd El-Rahman (2020);

3 – upwelling, i.e., transport of silicic acid and colloidal silica from deeper to shallower parts of a sedimentary basin (Hein and Parrish, 1987);

4 – volcanic activity as a principal source of a soluble form of orthosilicic acid for chert formation (Yool and Tyrrell, 2005), and additionally as a source of nutrients for the growth of siliceous biota, which has been inferred in different Paleozoic basins worldwide (Racki and Cordey, 2000);

5 – a hydrothermal sea-floor source of silica that led not only to formation of cherts, but also provided essential nutrients for sponge and radiolarian biota that occupied hydrothermal vent fields (Sharp et al., 2002; Migaszewski et al., 2006, 2022; Holzer et al., 2014; Kochman et al., 2020a, b);

* E-mail: meryem.yesilotkaplan@iste.edu.tr

Received: January 30, 2025; accepted: July 12, 2025; first published online: October 20, 2025

6 – other processes, for example a release of silica as a result of clay mineral transformations (e.g., [Metwally and Chesnokov, 2012](#)).

During the Eocene, there was an abundance of silica in sediments, increased marine biological productivity, and widespread silicification in some regions of the Earth (e.g., [Surdam et al., 1972](#); [Hein et al., 1990](#); [Shaaban, 2004](#); [Penman et al., 2019](#)). [Muttoni and Kent \(2007\)](#) proposed an excess of silica to explain the predominance of chert in the Eocene and observed that the highest number of chert nodules in studies throughout the Cenozoic were found in the warmest part of the Eocene. The chert layers of the Okçular Formation in Turkey and chert nodules were also formed during the Eocene ([Yeşilot Kaplan, 2023](#)).

This study determines the silicification of limestones in the Okçular Formation, the microstructural properties of chert forms, and the silicification stages of the region. The mineralogical changes of nodular and layered cherts with diagenetic, chemical and physical effects were investigated in detail.

GEOLOGICAL SETTING

The study area is located in a region that forms the boundary between the African, Eurasian and Arabian plates and is an area of active deformation between the Dead Sea Fault Zone, the East Anatolian Fault Zone and the Cyprus Arc. The Arabian and African plates moved northwards from the Cretaceous and came into collision with the Eurasian Plate. Miocene sediments associated with tectonic events from the Late Cretaceous to the present were deposited within the foreland basin. The Belen Fault, in contact with the Eocene and Upper Miocene deposits, developed in this area where ophiolitic rocks are observed as allochthons ([Fig. 1A](#); [Boulton and Robertson, 2007](#)).

Cenozoic units are deposited on the allochthonous Kızıldağ ophiolite basement rock of the Upper Cretaceous in the Belen (Hatay) region in Turkey ([Fig. 1A](#)). The middle-upper Eocene Okçular Formation, consisting of cherty limestone, limestone

and clastic limestone with moderately thick cherts was deposited in a shallow marine shelf environment on the Kızıldağ ophiolites.

The Okçular Formation consists of limestones rich in fossils, cherty limestones and clastic limestones. It consists of medium-to thick-bedded, locally massive, jointed, sharp-angled and fractured, hard limestones ([Ateş et al., 2004](#)). Carbonate beds reach 1 metre in thickness and are usually associated with chert layers. Silicification of carbonates is gradual and transitional to cherts, and microlaminations known as replacement markers are also distinguished.

MATERIAL AND METHODS

FIELDWORK AND SAMPLING

Layer thicknesses and nodule sizes of chert nodules and layers in the Okçular Formation were measured in the field, and samples were taken from chert nodules with and without rims, chert layers, and nodules associated with fractures. A total of 25 hand samples, including 10 layered chert, 10 chert nodules and 5 clay samples, were collected from the field for examination.

The geological Rock-Colour Chart prepared by the Geological Society of America (GSA) was used to determine the colour changes observed in the rims, nodules and limestones formed by silicification. [Table 1](#) summarizes the chert and limestone zones, colour codes and lithological features recorded.

SAMPLE PREPARATION AND ANALYSIS

Scanning electron microscopy-energy-dispersive spectrometry (SEM-EDS) device was used for imaging, measurement and analysis of silicification and changes in microstructure of limestones common in the Okçular Formation. Energy-dispersive spectrometry (EDS) measurement parameters on the

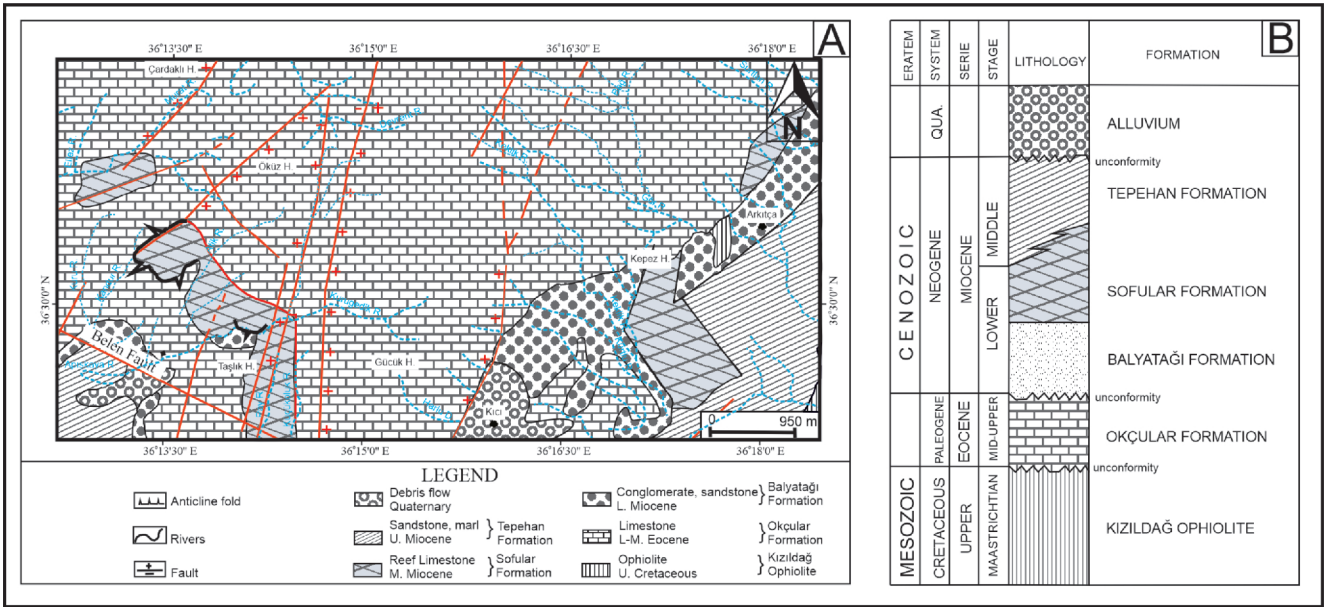
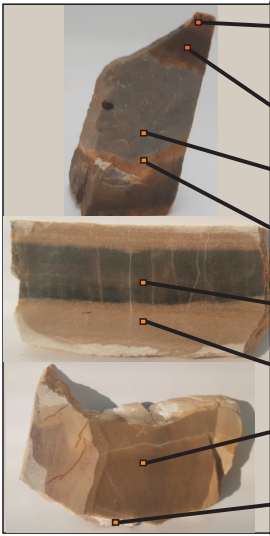


Fig. 1. Geological map of the Belen region ([Özşahin, 2013](#)) and a stratigraphic column

Table 1

Types of zone, sample and colour code in samples of nodular, fractured and layered chert

	Sample	Colour code	Type
	NX1	10YR 5/4	Outer cortex
	NC1	5GY 4/1	Dark grey chert
	NK1	N4	Grey cherty limestone
	NX2	10YR 6/6	Inner cortex
	NC2	5GY 4/1	Fractured grey chert
	NK2	5Y 7/6	Fractured cherty limestone
	NC3	N7	Layered chert
	NK3	5Y 7/6	Layered cherty limestone

Thermo Fisher Scientific Apreo S Scanning electron microscopy (SEM) device used were: voltage 15 kV under 10.3 working distance and 5000x magnification.

SEM analysis was performed to determine the effect of microquartz crystal size on chert colour and the porosity of the inner-outer rims in the nodules by image processing. Crack geometry, porosity, and grain/crystal sizes in the chert nodule layers and limestones were obtained from SEM images. Energy dispersive X-ray data were acquired from 5000x magnification images of areas of chert and limestone identified, and elemental changes were determined by replacement of carbonates.

RESULTS

DESCRIPTION OF CHERT OCCURRENCES

The cherts occur in three forms in the Okçular limestones: chert nodules with rims, chert bedding and fractured nodules. Microfossil remains preserved by silicification are common, especially of foraminifers a few centimetres across (i.e. small pebble size) scattered within the limestones (Fig. 2A). The cherty microfossils are grey, circular/oval in shape and their inner textures cannot be identified due to silicification.

The cracks in the limestone strata are both perpendicular and parallel to the bedding plane. It was found that there are crack infills of diagenetic silica present in those fractures that are oriented parallel to bedding (Fig. 2B). Chert nucleation of the nodules started in the cracks and chert nodules vary from 1–50 cm (Fig. 2C). The width of the cracks that have been filled with silica is greater than the widths of unfilled cracks (Fig. 2C, D). Well-developed chert nodules are typically observed alongside cracks that parallel to the earlier-formed bedding plane. (Fig. 2D–G).

Chert nodules developed independently of each other and their development directions are also different in well-developed nodules. Well-developed nodules show differences in po-

rosity, rim development and thickness. Light brown and porous silica accumulations are observed in the cracks together with the chert nodules in the carbonates (Fig. 2E).

There are chert nodules without rims, nodules with cortical and double rims, developed by silicification in the Belen carbonates. The outer rim of the nodules is light brown and has high porosity, the chert colour changes from light grey to dark grey as the degree of silicification increases towards the centre of the nodules. The outer rim and the centre of the nodule have a sharp transition, but gradual colour transitions are observed towards the centre of the nodule. The colour is dark grey in well-developed nodules and the rims becomes thinner as the nodules grow (Fig. 2D, E).

Folds due to tectonism are observed that post-date the formation of the nodules (Fig. 2F). There are stylolites in the limestones at the edges of the nodules due to the growth of the nodules (Fig. 2G). The limestones and chert features in the Okçular Formation are cut by cracks (Fig. 2H). The layered cherts and cracks seen in the region are parallel.

Changes occur in the form of the flint depending on the frequency of cracks. In thin or slightly fractured thick-bedded limestones, chert accumulations, small amorphous chert forms and silicified microfossils occur (Fig. 2A). If there are many pre-existing cracks in the formation, the growth size of chert nodules increases in direct proportion, and well-developed chert nodules can form.

MINERAL AND MICROTTEXTURAL CHARACTERIZATION OF THE CHERTS

PETROGRAPHY

The microtextures of the cherts in the Okçular Formation are related to the precursor limestones. The texture of limestones associated with chert nodules and layers is biomicritic. In limestones where planktonic and benthic foraminifera are abundant, micrite and calcite shells are replaced by quartz crystals

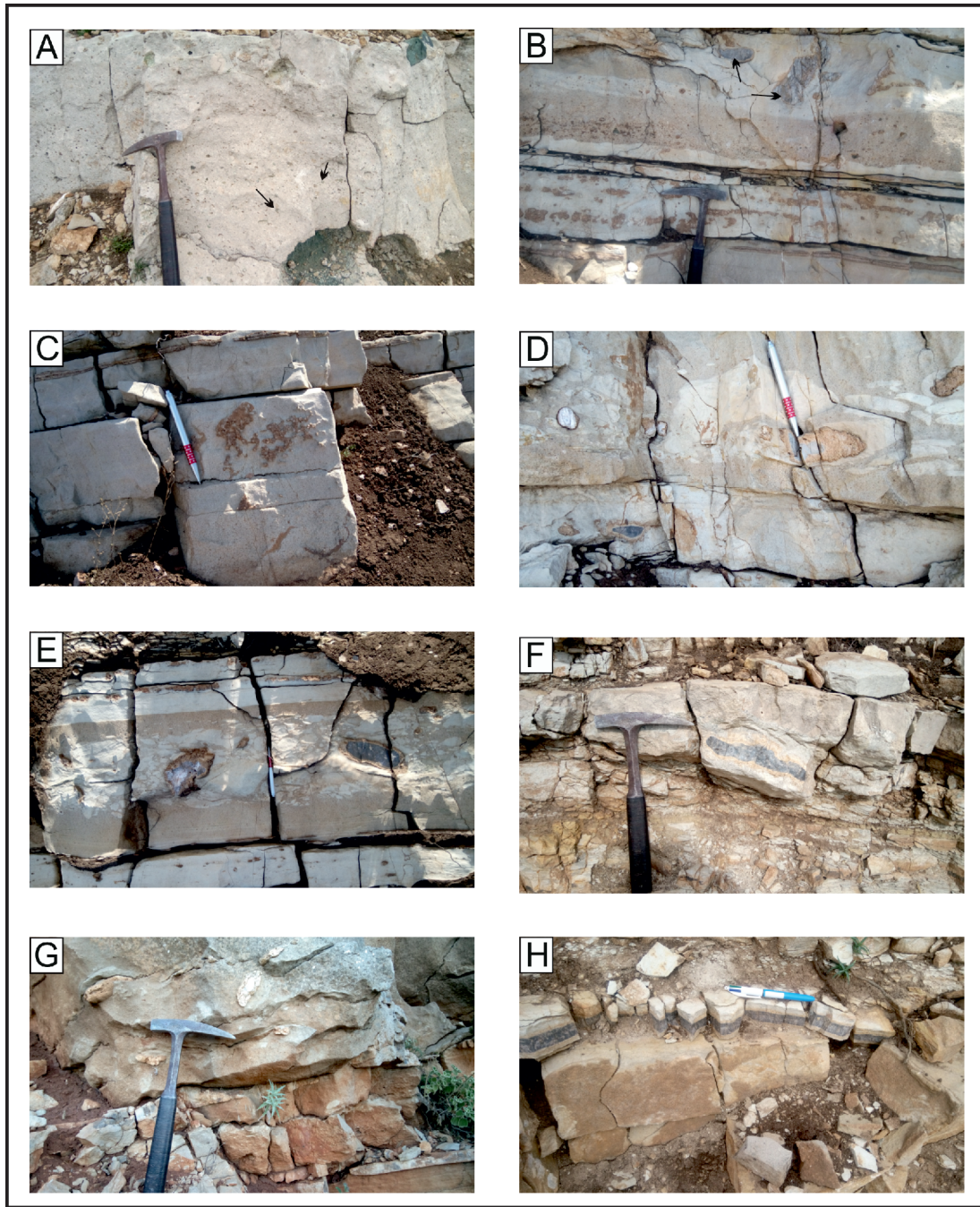


Fig. 2. Field observations of limestones and chert nodules

A – chert microfossils (arrowed) in the limestones, **B** – chert and nodules (arrowed) formed in the cracks, **C** – mat-like light brown chert in the cracks, **D** – size differences in the chert nodules, **E** – differences in the growth directions of the nodules, **F** – folding of nodules, **G** – stylolites associated with chert nodules, **H** – cutting of limestones and cherts by cracks

due to silicification. Microlaminations showing successions of calcite and quartz crystals are observed both in petrographic and field studies.

Scanning electron microscopy (SEM) analyses were performed on inner and outer rims, black-grey cherts and limestones to determine the silicification of the limestones and microtextural changes, cracks and porosities due to silicification and energy-dispersive spectrometry (EDS) measurements were performed on 5000X magnified fields to analyse the general chemical composition of these areas. SEM-EDS measure-

ments were made on layered, rimmed and non-rimmed fractured cherts and cream-coloured limestone/cherty limestone to examine the degree of silicification and crystal morphology, and it was determined that different elements were added to the rock in trace amounts during silicification.

SEM ANALYSIS

SEM analysis shows differences between the inner and outer rims and centres observed in well-developed chert nod-

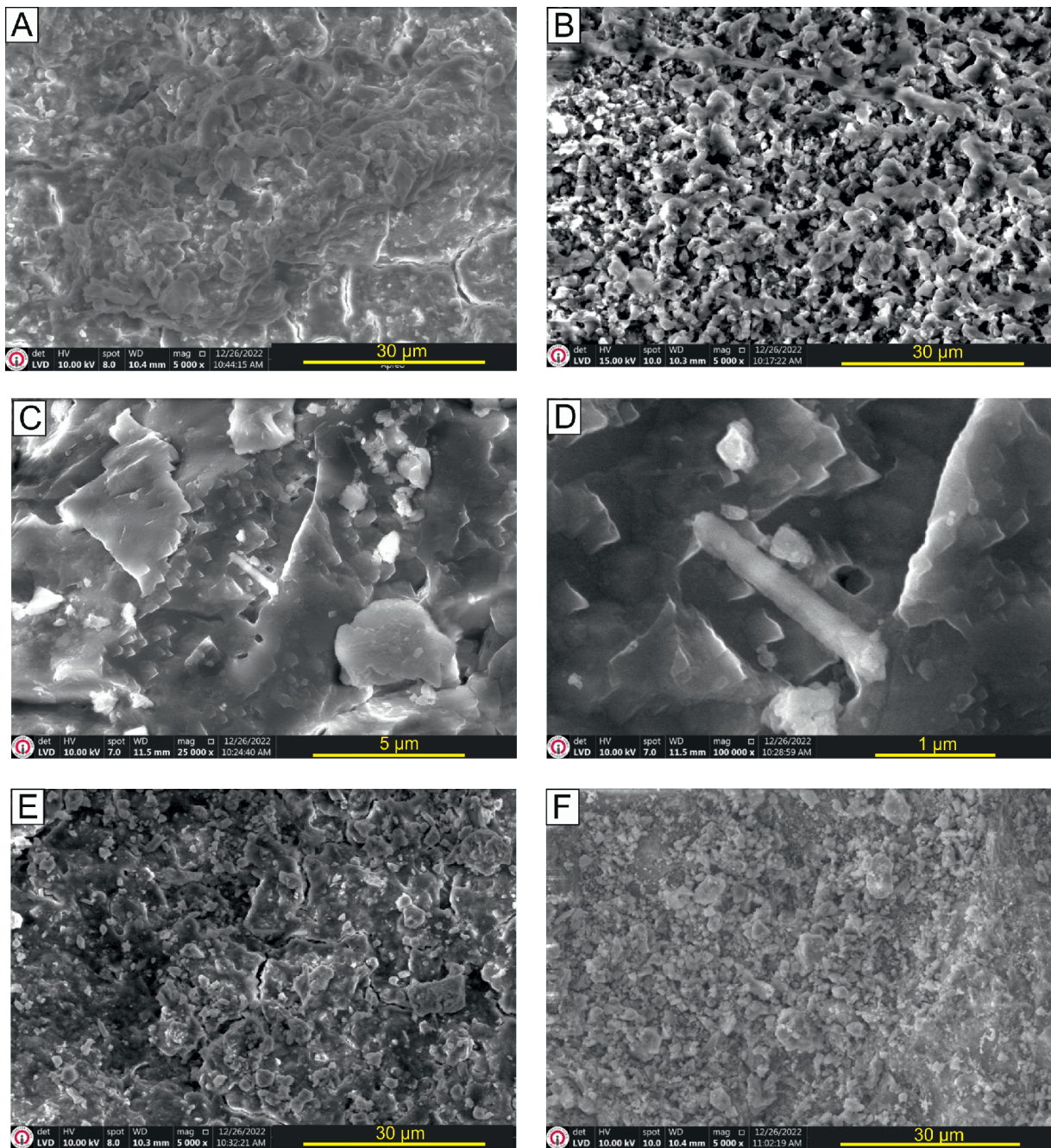


Fig. 3. SEM images of the Okçular Formation cherts

A – cracks and pores observed in the outer rim (NX1) from the double rims observed in the chert nodules, **B** – SEM image of the inner rim (NX2); **C** – anhydrous authigenic microquartz observed in the chert nodules, **D** – silicified bioclast remnants found in chertified limestone; **E** – microquartz and cracks in black cherts (NC1); **F** – microquartz crystallization in the direction of microlamination of the cherts

ules. Porosity and cracking are present in both the inner and outer rims and microquartz crystals are seen along pores and cracks (Fig. 3A, B).

Growth of the corners of the quartz crystals towards the crack spaces was observed. There is a mat-like texture in the inner and outer rim resulting from circulation patterns of siliceous fluids through cracks and pores in the dissolution-re-crystallization process.

Quartz crystals are anhedral in limestone silicification zones in the Okçular Formation (Fig. 3C). The silicification of lime-

stones resulted in the widespread occurrence of microquartz crystals, with a reduction in calcite crystals. Microcrystalline quartz crystals are present in the black zones of the chert nodules, together with bioclast remains from the precursor limestones (Fig. 3D). Silica overgrowth towards the crack cavities is observed on anhedral quartz crystals (Fig. 3E). SEM images reveal planar microlaminations (Fig. 3F).

The presence and orientation of cracks in the rim section (NX1–NX2) surrounding the nodules provides evidence that silica-rich fluid flow was directed towards the nodule cores (Fig.

SEM-EDS ANALYSIS AND TRACE ELEMENTS CONTENTS IN CHERTS

The elements Si, Ca, C, and O have been identified in both chert and limestone. In contrast, K, P, Ti, and Mn have been detected in nodule rims.

The porosity values measured by IMAGEJ in the scanning electron microscopy images obtained from the Okçular Formation cherts ranged from 18–20%, the maximum porosity being in the rims. These values are equivalent to the values measured by image processing of hand samples (Yeşilot Kaplan, 2023). Rim porosity depends on cracks.

Both the mat-like texture and porosity played a role in crystal development in the rims, and the pores and cracks in the quartz crystals are micro-sized. The longest calcite and quartz grains/crystals observed in clear SEM images were measured and their averages were taken. Accordingly, 74, 94, 65, 44, 56, 96, 46 and 59 numbers of crystal/grain lengths were measured.

Table 2

SEM-EDS element analysis data for nodular, fractured and layered cherts

[illegible]

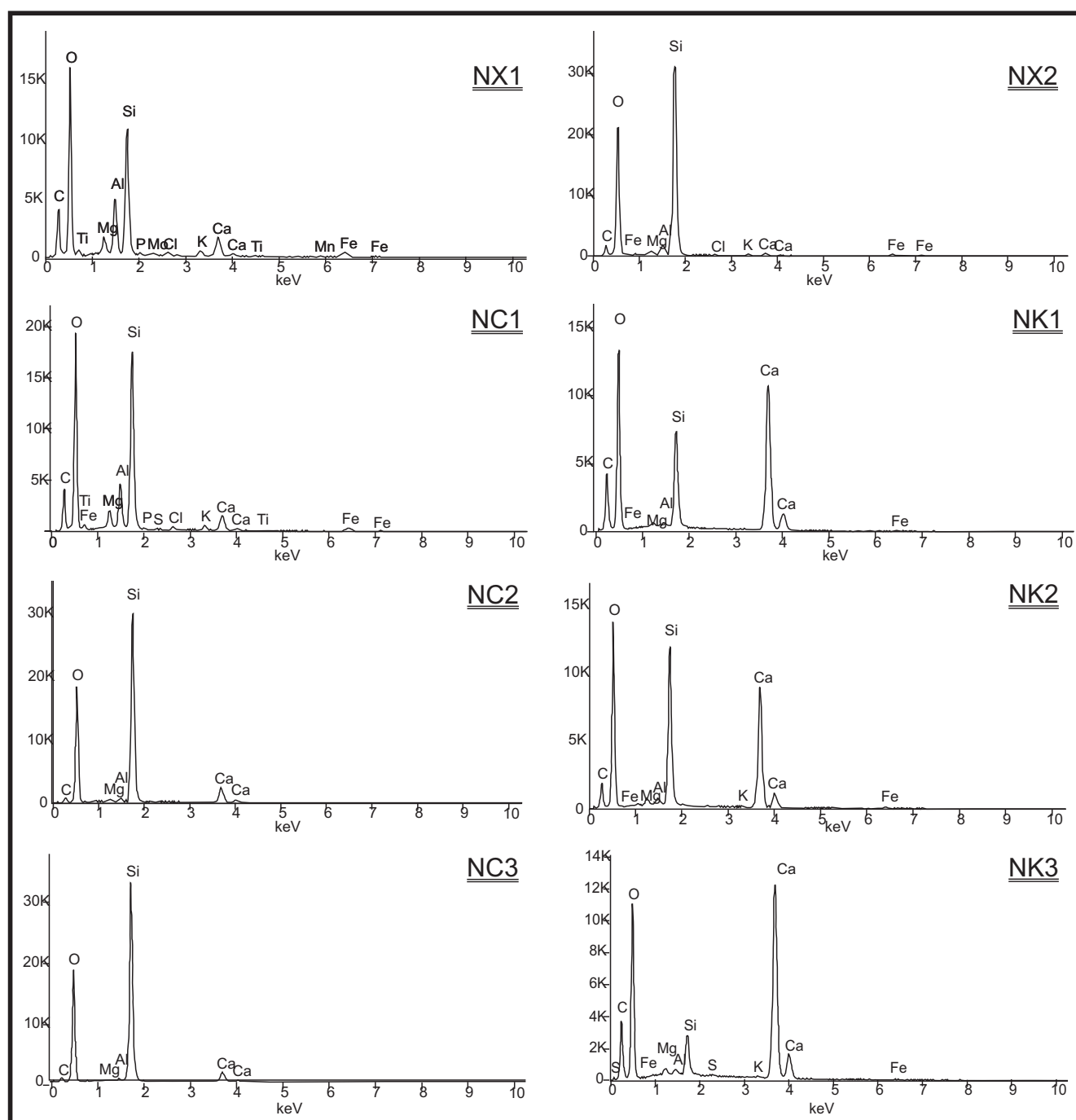


Fig. 4. Elemental composition changes in Okçular Formation cherts and limestones by EDS microanalysis

respectively from the NX1, NX2, NC1, NK1, NC2, NK2, NC3 and NK3 images. The average crystal/grain sizes in the limestones, cherts and rims are 1.17, 2.12 and 0.68 μ , respectively, and the primary grain sizes in the limestones are also related to silicification. The quartz crystals found in the cherts grew under the influence of siliceous fluids and colour changes occurred, from brown to grey and finally to black. Growths in crystal sizes are proportional in limestone and cherty limestones and cherts.

STYLOLITES

Two types of silicification-related stylolites were observed in the Belen carbonates:

- stylolites observed parallel to joints and bedding,
- diagenetic stylolites developed by the formation and growth of nodules.

The dimensions of the stylolites vary, ranging from micro to macro size. The stylolites in the Okçular Formation are paral-

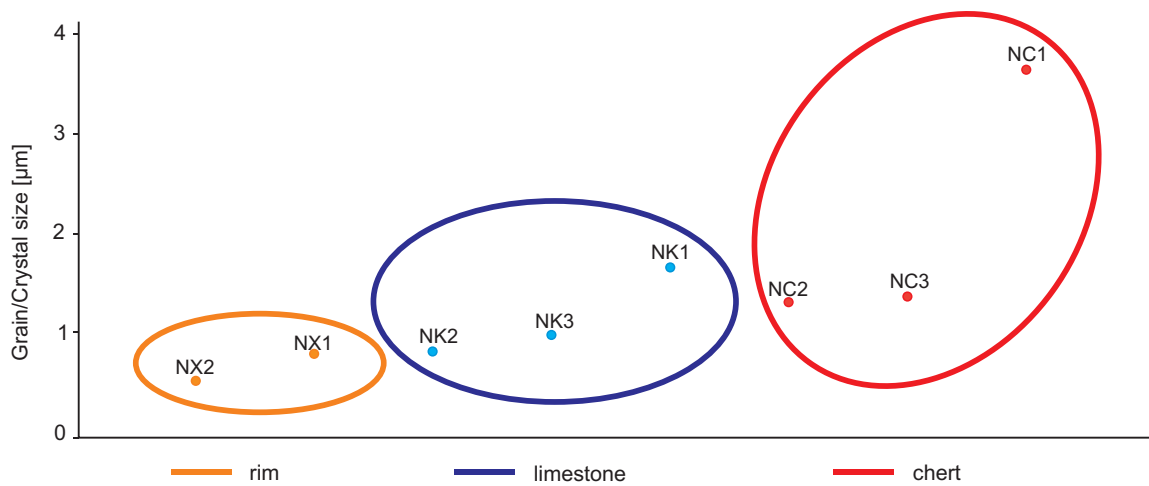


Fig. 5. Graph of grain sizes measured by imaging in limestones, rims and cherts

lel/semi-parallel to joints and bedding (Fig. 3C). In addition to stylolites formed by tectonic effects, stylolites are observed around the nodules as a result of replacement growth. Aase et al. (1996) suggested that stylolites inhibit the development of macrocrystalline quartz overgrowth. In the Okçular Formation, stylolites were also effective promoters of silicification. These stylolites are of low amplitude due to pressure dissolution and exhibit crack-like behaviour allowing fluid movement. Stylolites found together with well-developed nodules, and extending into the chert, are also observed. Field observations suggest that stylolites have the function of enhancing siliceous fluid transport in all chert forms through joints (Fig. 2G).

INTERPRETATION AND DISCUSSION

INTERPRETATION

Silicification in the Okçular Formation is associated with joints parallel to the bedding planes in the carbonates, due to the circulation of siliceous water along these cracks. As the circular/elongated nodules grew, the cracks also widened, and the growth direction of the nodules is usually parallel to the direction of the main crack (Fig. 2D–G). Evidence that tectonism is effective in the deposition, diagenesis and silicification of the Okçular Formation is the fact that the carbonates and cherts are cut by joints (Fig. 2H). The chert deposits have nucleated and grown along the cracks, and the layered cherts are parallel to the cracks. Layered cherts have formed due to the abundance of cracks together with well-developed nodules (Fig. 2E). The occurrence of quartz crystal microlamination is attributable to silicification between the calcite crystals of the limestones (Fig. 3F). Stylolites related to the deposit and cracks formed by the effect of the regional tectonism played an effective role in this replacement process (Fig. 6B). The presence of expansion cracks and stylolites in the chert nodules and the observation of fabric-preserved silicification indicate that replacement growth was effective in the Okçular Formation.

The anhedrality of the quartz and the quartz overgrowth in petrographic (thin-section and SEM) images corroborate micro-quartz replacement and authigenic quartz crystallization. Differ-

ences in quartz crystal sizes indicate that, during the last stage, quartz microcrystals were replaced by larger quartz crystals. The preservation of both the texture of the host rock and the morphology of the silicified microfossils is indicative of replacement. The pore water oversaturation in silica in the marine environment, thus, led to selective replacement of the limestones. Evidence of replacement growth:

- chemical compound is silica in thin-sections where foraminiferal forms are intact;
- cracks and stylolites are observed in chert nodules due to expansion.

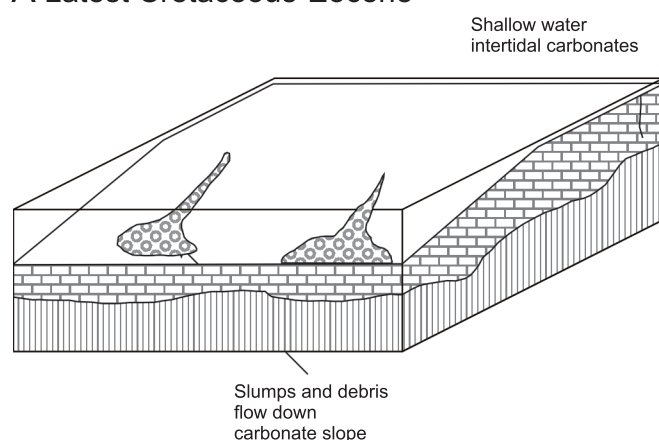
There is an allochthonous ophiolite which was a source of Si on the sea floor and is overlain by Okçular Formation limestones. Sea water was saturated with Si dissolved from the ophiolites and replacement has occurred within the Okçular Formation. Over time, layered and nodular cherts were formed in the limestones due to the dissolution of Si from the mafic units on the seabed.

Although not found in the nodule core, the mobility-specific elements K, P, Ti and Mn are thought to have been transported from areas where replacement is effective and concentrated in the rims. Si, Ca, C, and O are found in both chert and limestone, and their amounts vary with the level of replacement.

DISCUSSION

Replacement: the occurrence of replacement growth in cherts is characterized by the presence of irregular shapes and semi-fibrous internal microtextures. By contrast, displacive growth is distinguished by regular shapes and microcrystalline textures. Primary texture is not recognized in displacive growth and random crystallisation is common, whereas primary texture is preserved in replacive growth. Nodules exhibit either a replacive or displacive growth mode, the appearance of which is largely dependent on the original host lithology. Displacive nodules exhibit irregular shapes and semi-fibrous internal structures, in contrast to the regular shapes and microcrystalline textures observed for replacive nodules (Abu-Mahfouz et al., 2023). Internal structures and host lithology are preserved in nodules of the Okçular Formation.

A Latest Cretaceous-Eocene



B Eocene-Miocene

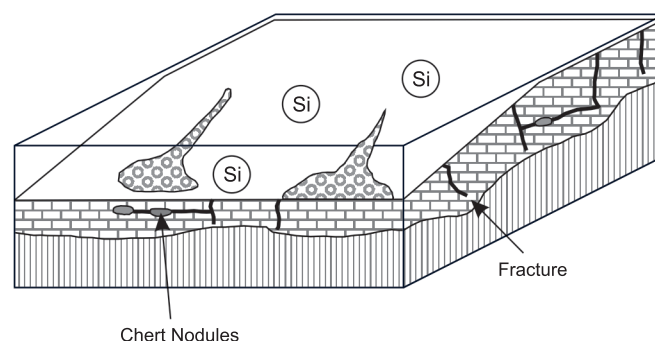


Fig. 6. Silicification model: A – Belen geology in the Late Cretaceous-Eocene (Boulton and Robertson, 2007); B – formation of chert nodules in the Okçular Formation

Dissolved silica-rich water partially replaces the calcite grains in the medium- to thick-bedded limestones of the Okçular Formation and chert was formed diagenetically (=post-depositionally) by silicification. Replacement and porosity in the development of the rim, which was most affected by the siliceous waters, are higher than in other forms of the nodules. Microlaminations occurred in the Okçular Formation as a result of silicification in the limestones, and these laminae show that silicification was active in the diagenetic stage prior to compaction (Xiao et al., 2010; Wen et al., 2016). Lamination and microlamination are observed in areas where large nodules could not develop in cherty limestones of the Okçular Formation (Fig. 3F). Microlaminations have formed with a sequence of silicified and limestone zones due to size and mineral differences of microquartz grains (Table 1, NK2). Replaceive nodules are those that display regular morphologies, ghosts of microfossils and infilled porosity, and well-preserved primary sedimentary structures and laminae within the nodule body. These characteristics indicate a replaceive growth mechanism (Maliva and Siever, 1988; Abu-Mahfouz et al., 2023).

Bioclasts known as carbonate allochems (e.g., foraminifers as microfossils and mollusks and echinoderms as macrofossils) are commonly silicified by replacement (Milliken et al., 2016). The shape of the quartz must have been formed by the displacement of skeletal parts; fossil forms are preserved but cannot be recognized because their internal structure is unclear. Fossil internal textures in the Belen carbonates are not clear, but foraminiferal forms are preserved. The initial replacement of fossils in the limestones is indicative of selective silicification, which suggests the presence of a marine environment.

There is a relationship between the size of the microquartz crystals and the colour of the cherts, depending on the fluid circulation, the amount of trace elements, and the degree of silicification. As the size of microquartz crystals increases due to all these factors, the colour changes from brown to grey-black.

Palaeoenvironment: SiO_2 is relatively high in the chemical composition of cherts and Si peaks are seen in SEM-EDS analysis. Along with SiO_2 , cherts may contain elements such as Al, Fe, Mn, Ca, Na, Mg, Ti and a few other elements such as the trace elements Ce, Eu and La (Boggs, 2012). Elements such as Fe, Mn, Ni and Cu precipitate from sea water or pore water in the formation of cherts. The presence of the elements Cl, P, Ti, Mn and Mo in the silicified limestones of the Okçular Formation

suggests precipitation of the cherts from sea water. The positive relationship between Fe and Si indicates the effect of submarine hydrothermal fluids (Murray, 1994). Fe decreases as silicon increases in the limestones of the Okçular Formation, the negative relationship between the two elements indicating a marine rather than hydrothermal effect. The absence of Mn, Ni and Co, which are indicators of anoxic environments, indicates that the Okçular Formation was deposited in an oxidizing environment.

There are many studies on the formation of nodules and/or chert layers through diagenetic replacement of carbonates due to the increase in silica in the seas during the Eocene (McBride et al., 1999; Suzuki et al., 2004; Abruzzese et al., 2005). Fossil and isotope data obtained from geological and climatic studies demonstrate that climatic temperatures increased during the Early Eocene, with ocean bottom water temperatures reaching a maximum of $\sim 50^\circ\text{C}$ (Muttoni and Kent, 2007). These conditions allowed for the dissolution of silica, which entered the ocean as a result of this extreme climatic heat. It has been hypothesised that silica may have been derived from continental weathering in the warmer and more humid climate that resulted from the accumulation of greenhouse gases in the atmosphere (Sloan and Rea, 1996; Pearson and Palmer, 2000). In the Okçular Formation silicification, it is thought that temperature-dependent dissolution was also involved in enhancing the Si source.

The effect of tectonism on silicification: all field, petrographic and chemical data show that the chert formation were early diagenetic and tectonism also played a role in the silicification. There is a direct relationship between the density of joints and the degree of silicification. In limestones with few cracks, silicification effects were small, whereas in limestones with many cracks, well-developed nodules can be seen. The development of silicification along the cracks indicates that the cracks formed in the pre-diagenetic limestones play a role in the transport of siliceous waters. The microlaminations are cut by the cracks, indicating that tectonism continued after silicification.

The SEM-EDS values from the nodules indicate that the silicification decreases from the outside to the inside, indicating that the extent of penetration of the silicification fluids depended on the cracks and pores in the limestones. Microquartz crystals fill the cracks, and nodules enlarged the cracks to form stress-based stylolites in the carbonates.

The absence of microorganisms such as radiolarians and sponges, which cause silicification, in the Okçular Formation indicates that cherts formed due to the input of inorganic silica. The mechanism of silicification in the Belen carbonates is the occurrence of silicification along the cracks following the formation of limestones as a first stage, the formation of silica nodules by expanding the cracks as a second stage, and the joints of both nodules and limestones as a third stage.

CONCLUSIONS

The Okçular Formation is characterized by the presence of cherts that were formed during the Eocene Epoch, a time marked by an increase in silicification on a global scale. The formation was exposed to the effects of marine silica waters due to the presence of cracks in the limestones, the predominant li-

thology of the formation. Silicification started during sedimentation in early diagenetic stages and lasted for a long time due to the effect of regional tectonism. The presence of silicification and replacement during sedimentation is indicated by microlaminations, grain size differences, primary texture preservation, overgrowth in quartz crystals, and chemical data. There are nodular, layered and fractured chert types in the formation due to the effect of silicic waters. The presence of the elements Cl, P, Ti, Mn and Mo in the limestones of the Okçular Formation provides evidence for the precipitation of cherts from sea water. A direct relationship has been demonstrated between the density of joints and the degree of silicification. The microlaminations are cut by the cracks, indicating that tectonism persisted following silicification.

Acknowledgements. I thank the three anonymous journal reviewers and the editor for helpful comments on an earlier draft.

REFERENCES

- Aase, N.E., Bjørkum, P.A., Nadeau, P.H., 1996. The effect of grain-coating microquartz on preservation of reservoir porosity. *AAPG Bulletin*, **80**: 1654–1673; <https://doi.org/10.1306/64EDA0F0-1724-11D7-8645000102C1865D>
- Abdel-Wahab, A., El-Younsy, A.R.M., 1999. Origin of spheroidal chert nodules, Drunka Formation (lower Eocene), Egypt. *Sedimentology*, **46**: 733–755; <https://doi.org/10.1046/j.1365-3091.1999.00253.x>
- Abruzzese, M.J., Waldbauer, J.R., Chamberlain, C.P., 2005. Oxygen and hydrogen isotope ratios in freshwater chert as indicators of ancient climate and hydrologic regime. *Geochimica et Cosmochimica Acta*, **69**: 1377–1390; <https://doi.org/10.1016/j.gca.2004.08.036>
- Abu-Mahfouz, I.S., Cartwright, J.A., Powell, J.H., Abu-Mahfouz, M.S., Podlaha, O.G., 2023. Diagenesis, compaction strain and deformation associated with chert and carbonate concretions in organic-rich marl and phosphorite; Upper Cretaceous to Eocene, Jordan. *Sedimentology*, **70**: 1521–1552; <https://doi.org/10.1111/sed.13085>
- Ateş, S., Kecer, M., Osmañelebioglu, R., Kahraman, S., 2004. Earth Science Data of Antakya (Hatay) City Center and Surroundings. MTA Institute, report no. 10717.
- Boggs, S., 2012. *Principles of Sedimentology and Stratigraphy*. Pearson, London.
- Boulton, S.J., Robertson, A.H., 2007. The Miocene of the Hatay area, S Turkey: transition from the Arabian passive margin to an underfilled foreland basin related to closure of the Southern Neotethys Ocean. *Sedimentary Geology*, **198**: 93–124; <https://doi.org/10.1016/j.sedgeo.2006.12.001>
- Clayton, C.J., 1986. The chemical environment of flint formation in Upper Cretaceous chalks. *Proceedings of the Fourth International Flint Symposium Held and Brighton Polytechnic*: 43–54. Cambridge University Press.
- Folk, R.L., Weaver, C.E., 1952. A study of the texture and composition of chert. *American Journal of Science*, **250**: 498–510; <https://doi.org/10.2475/ajs.250.7.498>
- Glock, W.S., 1920. The use of the terms flint and chert. *Proceedings of the Iowa Academy of Science*, **27**: 167–173.
- Heath, G.R., 1974. Dissolved silica and deep-sea sediments. *SEPM Special Publication*, **2**: 77–93; <https://doi.org/10.2110/pec.74.20.0077>
- Hein, J.R., Koski, R.A., 1987. Bacterially mediated diagenetic origin for chert-hosted manganese deposits in the Franciscan Complex, California Coast Ranges. *Geology*, **15**: 722–726. [https://doi.org/10.1130/0091-7613\(1987\)15<722:BMDOFC>2.0.CO;2](https://doi.org/10.1130/0091-7613(1987)15<722:BMDOFC>2.0.CO;2)
- Hein, J.R., Parrish, J.T., 1987. Distribution of siliceous deposits in space and time. *Siliceous Sedimentary Rock-Hosted Ores and Petroleum* (ed. J.R. Hein): 10–57. Van Nostrand Reinhold, New York.
- Hein, J.R., Yeh, H.W., Barron, J.A., 1990. Eocene diatom chert from Adak Island, Alaska. *Journal of Sedimentary Research*, **60**: 250–257. <https://doi.org/10.1306/212F9165-2B24-11D7-8648000102C1865D>
- Holzer, M., Primeau, F.W., DeVries, T., Matear, R., 2014. The Southern Ocean silicon trap: data-constraint estimates of regenerated silicic acid trapping efficiencies, and global transport paths. *Journal of Geophysical Research-Oceans*, **119**: 313–331; <https://doi.org/10.1002/2013JC009356>
- Hussein, A.W., Abd El-Rahman, Y.M., 2020. Origin of chert within the Turonian carbonates of Abu Roash Formation, Abu Roash area, Egypt: Field, petrographic, and geochemical perspectives. *Geological Journal*, **55**: 2805–2833 <https://doi.org/10.1002/gj.3566>
- Jurkowska, A., Świerczewska-Gładysz, E., 2020. Evolution of Late Cretaceous Si cycling reflected in the formation of siliceous nodules (flints and cherts). *Global and Planetary Change*, **195**, 103334; <https://doi.org/10.1016/j.gloplacha.2020.103334>
- Kastner, M., 1981. Authigenic silicates in deep-sea sediments; formation and diagenesis. *The Oceanic Lithosphere*, **7**: 915–980.
- Knauth, L.P., Epstein, S., 1976. Hydrogen and oxygen isotope ratios in nodular and bedded cherts. *Geochimica et Cosmochimica Acta*, **40**: 1095–1108; [https://doi.org/10.1016/0016-7037\(76\)90051-X](https://doi.org/10.1016/0016-7037(76)90051-X)
- Kochman, A., Kozłowski, A., Matyszkiewicz, J., 2020a. Epigenetic siliceous rocks from the southern part of the Kraków-Częstochowa Upland (Southern Poland) and the relation to Upper Jurassic early diagenetic chert concretions. *Sedimentary Geology*, **401**, 105636; <https://doi.org/10.1016/j.sedgeo.2020.105636>
- Kochman, A., Matyszkiewicz, J., Wasilewski, M., 2020b. Siliceous rocks from the southern part of the Kraków-Częstochowa Upland (Southern Poland) as potential raw materials in the manufacture of stone tools – a characterization and possibilities of identification. *Journal of Archaeological Science Reports*, **30**, 102195; <https://doi.org/10.1016/j.jasrep.2020.102195>
- Laschet, C., 1984. On the origin of cherts. *Facies*, **10**: 257–289. <https://doi.org/10.1007/BF02536693>

- Luedtke, B.E., 1992.** An Archaeologist's Guide to Chert and Flint. Archaeological Research Tools, vol. 7. Institute of Archaeology, University of California, Los Angeles.
- Maliva, R.G., Siever, R., 1988.** Mechanism and controls of silicification of fossils in limestones. *The Journal of Geology*, **96**: 387–398; <https://doi.org/10.1086/629235>
- Maliva, R.G., Siever, R., 1989.** Nodular chert formation in carbonate rocks. *The Journal of Geology*, **97**: 421–433; <https://doi.org/10.1086/629320>
- Mcbride, E.F., Abdel-Wahab, A., El-Younsy, A.R.M., 1999.** Origin of spheroidal chert nodules, Drunka Formation (lower Eocene), Egypt. *Sedimentology*, **46**: 733–755; <https://doi.org/10.1046/j.1365-3091.1999.00253.x>
- Metwally, Y.M., Chesnokov, E.M., 2012.** Clay mineral transformation as a major source for authigenic quartz in thermo-mature gas shale. *Applied Clay Science*, **55**: 138–150; <https://doi.org/10.1016/j.clay.2011.11.007>
- Migaszewski, Z.M., Gałuszka, A., Durakiewicz, T., Starnawska, E., 2006.** Middle Oxfordian–Lower Kimmeridgian chert nodules in the Holy Cross Mountains, south-central Poland. *Sedimentary Geology*, **187**: 11–28; <https://doi.org/10.1016/j.sedgeo.2005.12.003>
- Migaszewski, Z.M., Gałuszka, A., Migaszewski, A., 2022.** Geochemistry and petrology of striped cherts as a provenance tool for artefacts from the Krzemionki Neolithic mining area (Poland). *Archaeometry*, **64**: 1093–1109; <https://doi.org/10.1111/arcm.12778>
- Milliken, K.L., Ergene, S.M., Ozkan, A., 2016.** Quartz types, authigenic and detrital, in the Upper Cretaceous Eagle Ford Formation, south Texas, USA. *Sedimentary Geology*, **339**: 273–288; <https://doi.org/10.1016/j.sedgeo.2016.03.012>
- Murray, R.W., 1994.** Chemical criteria to identify the depositional environment of chert: general principles and applications. *Sedimentary Geology*, **90**: 213–232; [https://doi.org/10.1016/0037-0738\(94\)90039-6](https://doi.org/10.1016/0037-0738(94)90039-6)
- Muttoni, G., Kent, D.V., 2007.** Widespread formation of cherts during the early Eocene climate optimum. *Palaeogeography, Palaeoclimatology, Palaeoecology*, **253**: 348–362; <https://doi.org/10.1016/j.palaeo.2007.06.008>
- Özşahin, E., 2013.** Geomorphology of Belen Perched Synclines–Amanos Mountain. *The Journal of Academic Social Science Studies*, **6**: 1013–1036; <https://doi.org/10.9761/JASSS769>
- Pearson, P.N., Palmer, M.R., 2000.** Atmospheric carbon dioxide concentrations over the past 60 million years. *Nature*, **406**: 695–699; <https://doi.org/10.1038/35021000>
- Penman, D.E., Keller, A., D'haenens, S., Kirtland Turner, S., Hull, P.M., 2019.** Atlantic deep-sea cherts associated with Eocene hyperthermal events. *Paleoceanography and Paleoclimatology*, **34**: 287–299; <https://doi.org/10.1029/2018PA003503>
- Racki, G., Cordey, F., 2000.** Radiolarian palaeoecology and radiolarites: is the present the key to the past. *Earth-Science Reviews*, **52**: 83–120; [https://doi.org/10.1016/S0012-8252\(00\)00024-6](https://doi.org/10.1016/S0012-8252(00)00024-6)
- Shaaban, M.N., 2004.** Diagenesis of the lower Eocene Thebes Formation, Gebel Rewagen area, Eastern Desert, Egypt. *Sedimentary Geology*, **165**: 53–65; <https://doi.org/10.1016/j.sedgeo.2003.11.004>
- Sharp, Z.D., Durakiewicz, T., Migaszewski, Z.M., Atudorei, V.N., 2002.** Antiphase hydrogen and oxygen isotope periodicity in chert nodules; Implications for thermal instabilities in sedimentary basins. *Geochimica et Cosmochimica Acta*, **66**: 2865–2973; <https://doi.org/10.1086/626804>
- Siever, R., 1962.** Silica solubility, 0°–200°, and the diagenesis of siliceous sediments. *The Journal of Geology*, **70**: 127–150; <https://doi.org/10.1086/626804>
- Sloan, L.C., Rea, D.K., 1996.** Atmospheric carbon dioxide and early Eocene climate: A general circulation modeling sensitivity study. *Palaeogeography, Palaeoclimatology, Palaeoecology*, **119**: 275–292; [https://doi.org/10.1016/0031-0182\(95\)00012-7](https://doi.org/10.1016/0031-0182(95)00012-7)
- Surdam, R.C., Eugster, H.P., Mariner, R.H., 1972.** Magadi-type chert in Jurassic and Eocene to Pleistocene rocks, Wyoming. *GSA Bulletin*, **83**: 2261–2266; [https://doi.org/10.1130/0016-7606\(1972\)83:2261-2266](https://doi.org/10.1130/0016-7606(1972)83:2261-2266)
- Suzuki, H., Maung, M., Aung, A.K., Takai, M., 2004.** Jurassic radiolaria from chert pebbles of the Eocene Pondaung Formation, central Myanmar. *Neues Jahrbuch für Geologie und Paläontologie Abhandlungen*, **231**: 369–393; <https://doi.org/10.1127/njgpa/231/2004/369>
- Tréguer, P., Nelson, D.M., Van Bennekom, A.J., DeMaster, D.J., Leynaert, A., Queguiner, B., 1995.** The silica balance in the world ocean: a reestimate. *Science*, **268**: 375–379; <https://doi.org/10.1126/science.268.5209.375>
- Walker, T.R., 1962.** Reversible nature of chert-carbonate replacement in sedimentary rocks. *GSA Bulletin*, **73**: 237–242; [https://doi.org/10.1130/0016-7606\(1962\)73\[237:RNOCRI\]2.0.CO;2](https://doi.org/10.1130/0016-7606(1962)73[237:RNOCRI]2.0.CO;2)
- Wen, H., Fan, H., Tian, S., Wang, Q., Hu, R., 2016.** The formation conditions of the early Ediacaran cherts, South China. *Chemical Geology*, **430**: 45–69; <https://doi.org/10.1016/j.chemgeo.2016.03.005>
- Xiao, S., Schiffbauer, J.D., McFadden, K.A., Hunter, J., 2010.** Petrographic and SIMS pyrite sulfur isotope analyses of Ediacaran chert nodules: implications for microbial processes in pyrite rim formation, silicification, and exceptional fossil preservation. *Earth and Planetary Science Letters*, **297**: 481–495; <https://doi.org/10.1016/j.epsl.2010.07.001>
- Yeşilot Kaplan, M., 2023.** Geochemical, mineralogical and diagenetic characteristics of marine chert in the Hatay region, S-Turkey: its origin and depositional environment. *Carpathian Journal of Earth and Environmental Sciences*, **18**: 65–77; <https://doi.org/10.26471/cjees/2023/018/241>
- Yool, A., Tyrrell, T., 2005.** Implications for the history of Cenozoic opal deposition from a quantitative model. *Palaeogeography, Palaeoclimatology, Palaeoecology*, **218**: 239–255; <https://doi.org/10.1016/j.palaeo.2004.12.017>